

Enantioselective Total Syntheses of Cassane Furanoditerpenoids and their Stimulation of Cellular Respiration in Brown Adipocytes

Hendrik H. Bulthaupt,^a Fabian Glatz,^a Sven M. Papidocha,^a Chunyan Wu,^b Shawn Teh,^a Susanne Wolfrum,^a Lucia Balážová,^c Christian Wolfrum,^b Erick M. Carreira^{a*}

^a ETH Zurich, Vladimir-Prelog-Weg 3, HCI, 8093 Zurich, Switzerland; ^b ETH Zurich, Schorenstrasse 16, IFN, 8603 Schwerzenbach, Switzerland; ^c Biomedical Research Center of the Slovak Academy of Sciences, Bratislava, Slovakia

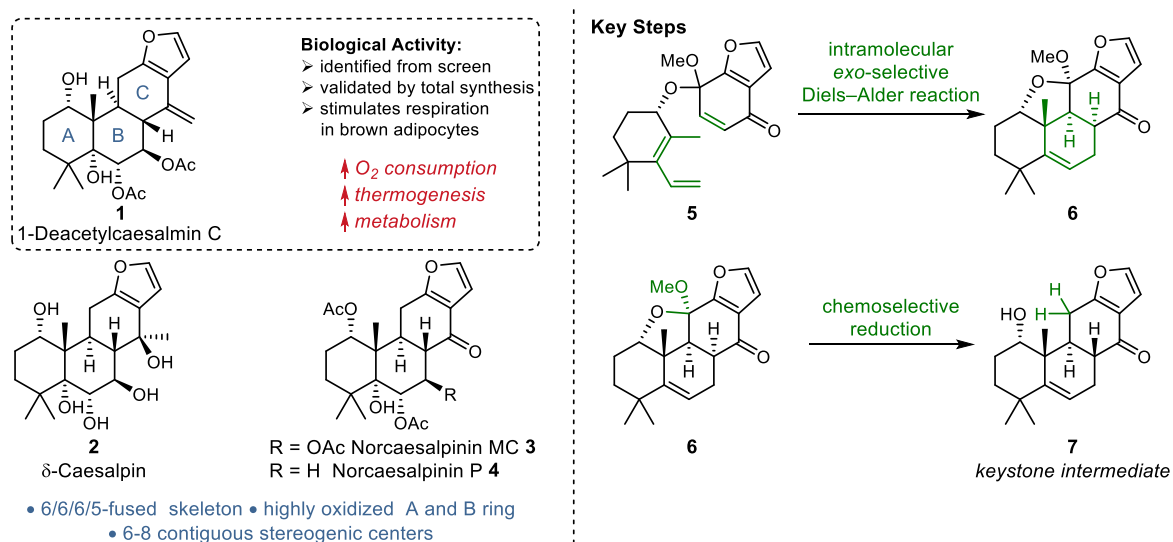
*E-Mail: erickm.carreira@org.chem.ethz.ch

Abstract

We report the first and enantioselective total syntheses of (+)-1-deacetylcaesalmin C, (+)- δ -caesalpin, (+)-norcaesalpinin MC, and (+)-norcaesalpinin P. Salient features of the synthetic strategy are *exo*-selective intramolecular Diels–Alder reaction of a furanoquinone monoketal and subsequent chemoselective reduction of the resulting pentacyclic furfuryl ketal furnishing a keystone intermediate. The latter enables access to the collection of natural products through implementation of stereoselective oxidations. Having accessed the cassane furanoditerpenoids, we unveil previously unknown bioactivity: (+)-1-Deacetylcaesalmin C stimulates respiration in brown adipocytes, which has been suggested to play a central role in treatment of obesity.

As part of our ongoing research program on metabolic disorders, specifically obesity, we have screened a library of natural products¹ to assess their effects on brown adipocyte metabolism through quantification of coupled and uncoupled cellular respiration rates. Among the more than 5000 secondary metabolites included in the screen, (+)-1-deacetylcaesalmin C (**1**)² stood out based on its ability to increase oxygen consumption (Scheme 1). The natural product belongs to the class of cassane-type furanoditerpenoids, which feature a 6/6/6/5-fused skeleton. (+)-1-Deacetylcaesalmin C (**1**) has seven contiguous stereogenic centers, one of which is quaternary. To date, no syntheses of cassane furanoditerpenoids with highly oxidized A and B rings have been documented.^{3,4} Herein, we report the first and enantioselective total synthesis of (+)-1-deacetylcaesalmin C (**1**) and data indicating stimulation of coupled and uncoupled respiration in brown adipocytes (Scheme 1). Highlights of the synthesis include *exo*-selective intramolecular Diels–Alder reaction of a furanoquinone monoketal and chemoselective Birch reduction. Elaboration of keystone intermediate **7** leads to the natural products (+)-1-deacetylcaesalmin C (**1**), (+)- δ -caesalpin (**2**),^{5, 6, 7} (+)-norcaesalpinin MC (**3**)⁸ and (+)-norcaesalpinin P (**4**).⁹

Scheme 1. 1-Deacetylcaesalpin (1), δ -Caesalpin (2), Norcaesalpinin MC (3), Norcaesalpinin P (4) and Key Steps

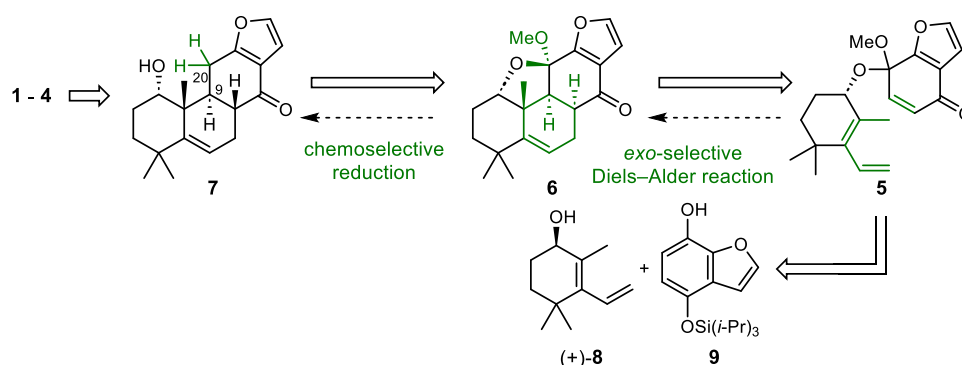


Obesity has been associated with several co-morbidities including type 2 diabetes, cardiovascular disease, musculoskeletal disorders such as osteoarthritis, and certain types of cancer.¹⁰ Thus, its prevention and treatment is of high importance. Pharmacological approaches are limited and several anti-obesity drugs have been developed but not approved due to side effects.^{11,12} An approach for treatment of obesity involves changes in lifestyle, but long-term compliance is poor.¹³ The adipose organ is a multi-depot endocrine organ that can be divided into white and brown adipose tissue.¹⁴ White adipose tissue (WAT) constitutes the major storage depot of excess energy in the form of

triacylglycerols. The primary function of brown adipose tissue (BAT) is non-shivering thermogenesis, or heat production. BAT is a promising therapeutic target to ameliorate obesity based on its increased number of mitochondria which upon stimulation can consume high levels of energy.

We designed a general, enantioselective strategy to access various cassane furanoditerpenoids, enabling the exploration of their biological activity. The retrosynthetic analysis of the targets leads back to **7** as a versatile keystone intermediate (Scheme 2). The ketone in **7** was anticipated to stabilize the otherwise oxidation-prone furan¹⁵ and suggests a Diels–Alder disconnection. The *anti*-relationship between the C20 methyl group and the proton at C9 implicates *exo*-selective Diels–Alder reaction. For related substrates *exo*-selectivities were only observed in intramolecular DA cycloadditions. Synthetic studies towards (±)-forskolin described DA reaction of the ester of (±)-**8** and maleic acid to afford the product in an *endo:exo*-selectivity of 1:3 in 56% yield.¹⁶ In addition, intramolecular DA reactions of simple, acyclic dienes tethered to protected *p*-benzoquinones have been described with *endo:exo*-selectivity of up to 1:1.¹⁷ We envisioned tethering a furanoquinone to enantioenriched allylic alcohol (+)-**8**¹⁸ via a ketal as shown in **5** and sought to evaluate its feasibility in a DA reaction. Although this transformation would provide rapid access to the tetracyclic carbon skeleton common to all cassane furanoditerpenoids, we were cognizant of a number of challenges. 1) Allylic alcohol **8** is prone to elimination resulting in a triene.¹⁹ 2) The presence of a *gem*-dimethyl group renders the diene sterically encumbered. 3) The rigidity imposed by the system might impede adoption of the necessary *S-cis* conformation. 4) While the ketal tether could enable *exo*-selectivity its subsequent removal requires chemoselective reduction.

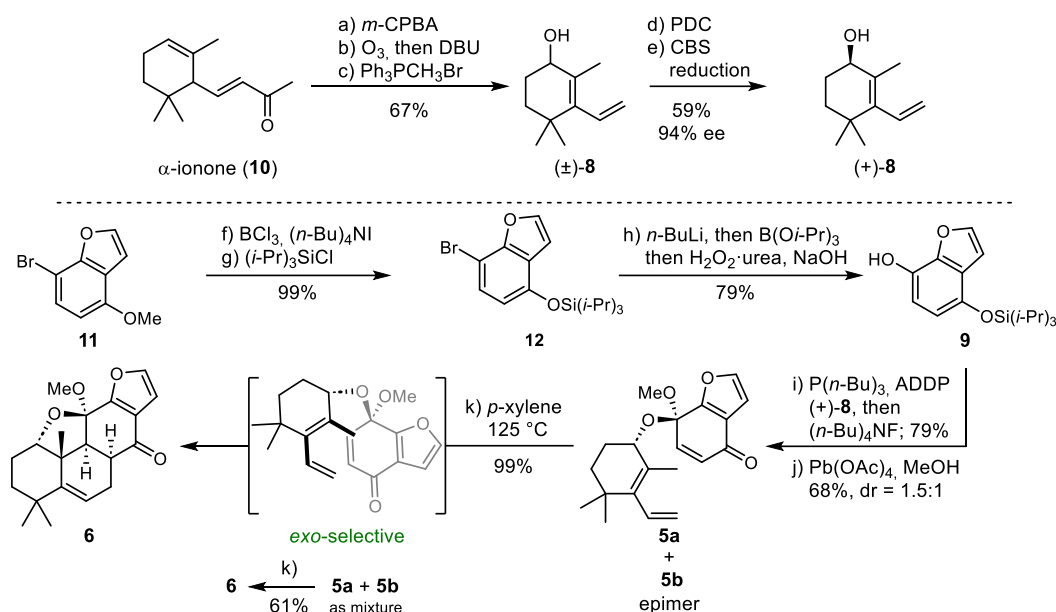
Scheme 2. Retrosynthetic Analysis



The synthesis commenced with preparation of enantioenriched allylic alcohol **8** via an adapted literature procedure (Scheme 3).^{18,20} Epoxidation of α -ionone (**10**) and subsequent ozonolysis gave the corresponding aldehyde, which was treated with DBU to afford the enal in one pot. Wittig olefination provided diene (±)-**8** in an overall yield of 67% over 3 steps. Oxidation with pyridinium dichromate (PDC) followed by Corey–Bakshi–Shibata (CBS) reduction yielded (*R*)-diene (+)-**8** in 59% yield and 94% ee over two steps.

Commercially available bromide **11** was demethylated with BCl_3 in the presence of (*n*-Bu)₄NI and the resulting phenol was protected as the silyl ether using (*i*-Pr)₃SiCl and imidazole (99% yield over 2 steps). Lithium–bromine exchange and subsequent transmetalation with $\text{B}(\text{O}i\text{-Pr})_3$ gave the boronic ester. Oxidation to the corresponding alcohol with H_2O_2 -urea and aq. NaOH provided alcohol **9** in 79% yield in one pot. Alcohols **8** and **9** were coupled using Tsunoda's modification of Mitsunobu reaction²¹ and the adduct subsequently desilylated in situ with (*n*-Bu)₄NF to afford the corresponding phenol in 79% yield. Oxidative dearomatization with $\text{Pb}(\text{OAc})_4$ gave enone **5** as a diastereomeric mixture of 1.5:1 (analyzed by ¹H NMR of the unpurified reaction mixture) in 68% yield and set the stage for the key Diels–Alder reaction.

Scheme 3. Synthesis of Diene 9, Phenol 8, and Key Intramolecular Diels–Alder Reaction

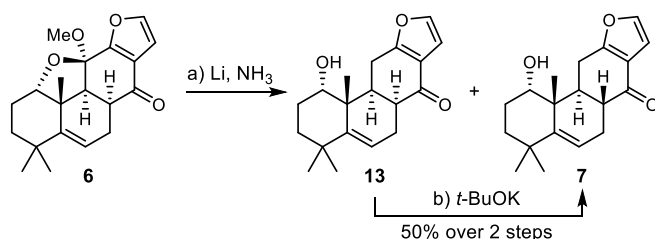


Reagents and conditions: (a) *m*-CPBA, CH₂Cl₂, 0 °C; (b) O₃, CH₂Cl₂, –78 °C, then Me₂S, –78 °C to rt, then DBU; (c) Ph₃PCH₃Br, *n*-BuLi, THF, 0 °C to rt (67% over 3 steps); (d) PDC, CH₂Cl₂, 4 Å MS (99%); (e) (*S*)-CBS catalyst, BH₃·SMe₂, PhMe–THF (1.1:1), 35 °C (58%, 94% ee); (f) BCl₃, (*n*-Bu)₄Nl, CH₂Cl₂, –78 °C to rt; (g) (*i*-Pr)₃SiCl, imidazole, CH₂Cl₂ (99% over 2 steps); (h) *n*-BuLi, B(O*i*-Pr)₃, THF, –78 °C to rt, then H₂O₂·urea, aq. NaOH (79%); (i) (+)-8, P(*n*-Bu)₃, ADDP, THF, 0 °C, then (*n*-Bu)₄NF (79%); (j) Pb(OAc)₄, MeOH, –78 °C (68%, dr = 1.5:1); (k) *p*-xylene, 125 °C (99%); **5a** + **5b** as mixture (61%); ADDP = 1,1'-(azodicarbonyl)dipiperidine.

Heating the diastereomeric mixture of **5** to 125 °C in *p*-xylene led to formation of DA product **6** as a single diastereomer in 61% yield whose configuration was determined as *exo* on the basis of NOESY experiments (Scheme 3). To understand the stereochemical course of the reaction and its outcome, diastereomers of **5** (**5a** and **5b**) were separated by preparative TLC and subsequently submitted to the DA reaction conditions independently. Interestingly, under the reaction conditions **5b** decomposed to a complex mixture of products, while **5a** quantitatively afforded **6**. Given the moderate selectivity in previous substrates for simple acyclic dienols, the observed stereochemical outcome in our study can be understood to arise from the constraints imposed by the *gem*-dimethyl substituted cyclohexene in combination with the methyl ketal stereogenic center.²²

Following successful DA cycloaddition reaction the next challenge was conversion of **6** to keystone intermediate **7** (Scheme 4). It is important to note that chemoselective reduction of ketal → CH₂ adjacent to furans, in the presence of ketones has not been investigated.^{23,24} We hypothesized that such a transformation could conceivably be conducted under dissolving metal conditions. Initial attempts under reported conditions (15 min, –78 °C)²⁴ resulted in formation of traces (<5%) of product. Increasing the reaction time to 30 min led to isolation of the corresponding product **13** (29%) and its epimer **7** (4%). We were pleased to observe epimerization of **13** to desired *trans*-decalin **7** under the reaction conditions. Treatment of isolated **13** with *t*-BuOK furnished **7** in 94% yield. Extensive optimization studies (see SI) revealed conditions prescribing warming to –33 °C over a period of 35 minutes and a subsequent quench at –78 °C. Under these conditions **7** was obtained after epimerization in 50% yield over 2 steps.

Scheme 4. Chemoselective Birch Reduction

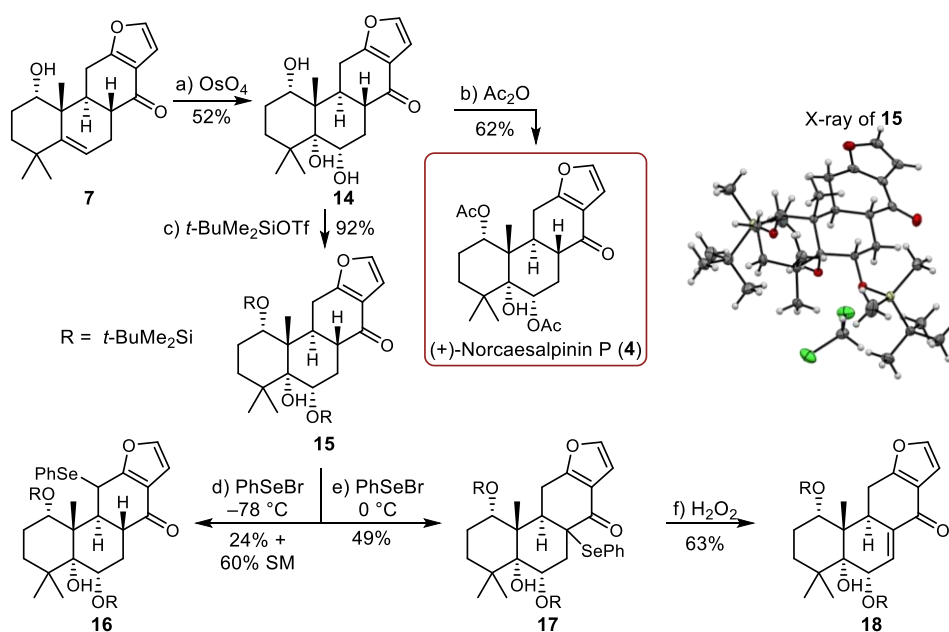


Reagents and conditions: (a) Li, NH₃ (l), –78 to –33 °C; (b) *t*-BuOK, *t*-BuOH (50% over 2 steps).

With a scalable route to keystone intermediate **7**, we turned our attention to the stereoselective introduction of the hydroxy and acetate groups contained in **1** - **4**. Initial attempts at allylic oxidation/dihydroxylation (CrO_3 or SeO_2 or CuBr) failed due to a number of side reactions: 1) elimination, 2) fragmentation, 3) aromatization.²⁵ The order of steps was reversed by first introducing the γ,δ -*syn*-diol followed by introduction of β -hydroxy group. Dihydroxylation of **13** with OsO_4 , NMO and DABCO gave **14** in 52% yield as a single diastereomer as indicated by analysis of the ^1H NMR spectrum of the unpurified reaction mixture (Scheme 5). Acetylation of **14** afforded **4**, whose analytical data (^1H NMR, ^{13}C NMR, IR, CD) matched those reported for (+)-norcaesalpin P.^{9,26} Silylation of triol **14** afforded the disilyl ether **15** in 92% yield as crystalline compound (X-ray). Selenylation of **15** using $\text{KN}(\text{SiMe}_3)_2$ and PhSeBr at -78°C gave γ -selenide **16** in 24% yield. We hypothesized that γ -enolate formation is kinetically controlled. Accordingly, in a subsequent experiment the enolization was conducted at 0°C followed by the addition of PhSeBr and α -selenide **17** was isolated in 49% yield. Treatment of **17** with H_2O_2 induced selenoxide elimination to afford enone **18** in 63% yield.

We considered 1,4-addition to enone **18** to access various organo -boranes and -silanes, that could be transformed oxidatively into a hydroxy group. 1,4-Addition with Lipshutz cyanocuprate $(\text{Me}_2\text{PhSi})_2\text{Cu}(\text{CN})\text{Li}_2$ ²⁷ afforded silane **19** in 84% yield as a single diastereomer (determined by analysis of the ^1H NMR spectrum of the unpurified reaction mixture) (Scheme 6). The relative configuration was assigned by NOESY experiments (for details see SI). The major product of a one-pot Fleming–Tamao oxidation (AcOOH , KBr , AcOH) was enone **18**. We speculated that acidic conditions lead to the elimination of the newly formed alcohol in β -position to the ketone.

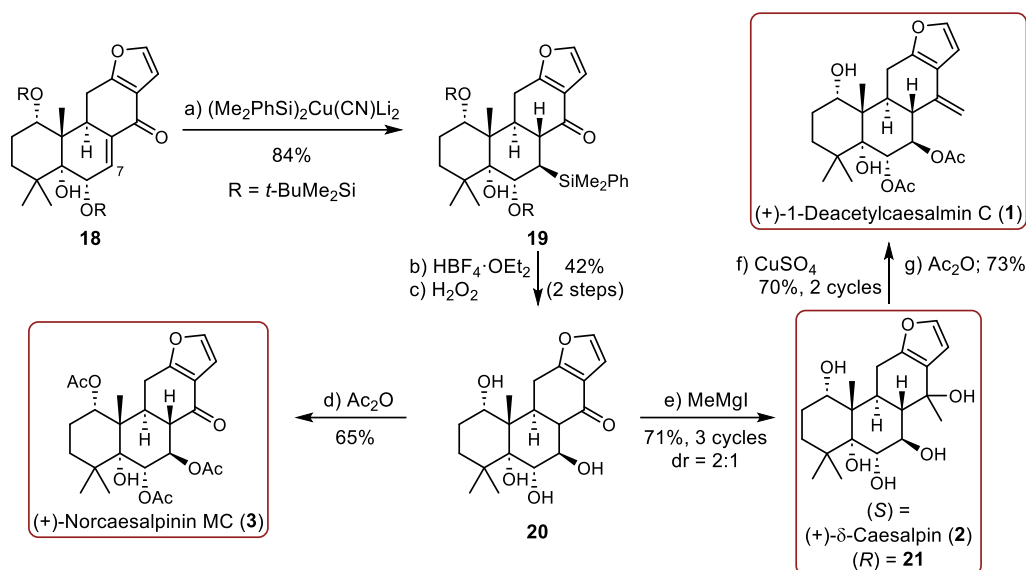
Scheme 5. Synthesis (+)-Norcaesalpin P (4) and Enone 18



Reagents and conditions: (a) OsO_4 , DABCO, NMO, acetone– H_2O (2:5:1), 90°C (52%); (b) Ac_2O , py, DMAP (61%); (c) $t\text{-BuMe}_2\text{SiOTf}$, 2,6-lutidine, CH_2Cl_2 (92%); (d) $\text{KN}(\text{SiMe}_3)_2$, -78°C then PhSeBr -78 to 0°C (24% + 60% SM); (e) $\text{KN}(\text{SiMe}_3)_2$, -78 to 0°C then PhSeBr , THF, 0°C (49%); (f) aq. H_2O_2 , CH_2Cl_2 – H_2O (20:1), 0°C (63%).

Consequently, the conditions were changed to a two-step Fleming–Tamao oxidation procedure where the second step involves mildly alkaline oxidizing conditions. Treatment of silane **19** with $\text{HBF}_4\cdot\text{OEt}_2$ led to silyl fluorination and concomitant desilylation of the alcohols. Keeping the temperature at -35°C was crucial because at higher temperatures Peterson elimination was observed. The silyl fluoride was then subjected to oxidation in the presence of KF , KHCO_3 and H_2O_2 -urea to afford tetraol **20** in 42% yield over 2 steps. Acetylation with DMAP, Ac_2O and pyridine gave (+)-norcaesalpin MC (**3**) in 65% yield. The spectroscopic data obtained of **3** (^1H NMR, ^{13}C NMR, $[\alpha]_D$, HRMS, IR) were in agreement with the reported data.^{8,28} 1,2-Addition of MeMgI to tetraol **20** afforded the corresponding pentaol in 35% yield and 2:1 dr along with 62% starting material. Resubjecting the starting material to the reaction conditions two more times gave the pentaol in 71% yield over 3 cycles. The major diastereomer was identified as (+)- δ -caesalpin (**2**), whose analytical data (^1H NMR, ^{13}C NMR) matched with literature precedent.^{6,7,29} Based on derivatization studies of Canonica and co-workers⁵, the mixture of **21** and **2** was dehydrated with CuSO_4 and gave the *exo*-methylene in 53% yield along with 45% starting material. Resubjecting the starting material to the reaction conditions gave the product in 70% yield over 2 cycles. The analytical data of the product (^1H NMR, ^{13}C NMR, HRMS) matched with the literature³⁰. Final regioselective acetylation with Ac_2O and pyridine afforded (+)-1-deacetylcaesalmin C (**1**) in 73% yield. The obtained analytical data (^1H NMR, ^{13}C NMR, $[\alpha]_D$, IR) were in agreement with the literature.^{2,31}

Scheme 6. Synthesis of (+)-1-Deacetylcaesalmin C (1), (+)- δ -Caesalpin (2) and (+)-Norcaesalpin MC (3)



Reagents and conditions: (a) $(\text{Me}_2\text{PhSi})_2\text{Cu}(\text{CN})\text{Li}_2$, THF, 0 °C to rt (84%); (b) $\text{HBF}_4 \cdot \text{OEt}_2$, CH_2Cl_2 , –35 °C; (c) KF , KHCO_3 , H_2O_2 -urea, THF–MeOH (1:1), 0 °C to rt (42% over 2 steps); (d) Ac_2O , py, DMAP (65%); (e) MeMgI , Et_2O (35%, dr = 2:1, 62% SM, 71% over 3 cycles); (f) CuSO_4 , 1,4-dioxane (53%, 45% SM, 70% over 2 cycles); (g) Ac_2O , py (73%).

We next set out to investigate the effect of **1** – **4** on the metabolism in brown adipocytes. Cellular oxygen consumption rates (OCRs) are directly linked to mitochondrial electron transfer and thus serve as useful measure for quantification.³² The mitochondrial electron transfer is coupled to proton transfer across the inner membrane, creating a proton gradient, which is utilized for ATP synthesis (coupled respiration) or for heat production (uncoupled respiration) mediated by Uncoupling Protein 1 (UCP1).^{33,34,14} OCRs can be assessed using the Seahorse XF96 method (Figure 1).³² Murine brown adipocytes (iBAs) were treated with DMSO (black) as a control and synthetic **1** (10 μM , red) for three days, respectively. Then, OCR was measured over a period of 18 min to yield 273 ± 17 – 248 ± 17 pmol/min for cells treated with synthetic **1** and 227 ± 4 – 203 ± 3 pmol/min for cells treated with DMSO (Figure 1A). These values represent the sum of basal mitochondrial (■+▨ for **1** and ▨ for control) and non-mitochondrial respiration (■). Basal mitochondrial respiration (■ and ▨) in turn is the sum of ATP synthesis-coupled and -uncoupled respiration processes. To determine the OCR of each process, the cells were then treated with 2.5 μM oligomycin (Oligo), which suppresses ATP-synthesis. This led to a reduction of OCR by 74 ± 10 – 70 ± 9 pmol/min for **1** and 61 ± 3 – 52 ± 3 pmol/min for control, which corresponds to the contribution of ATP synthesis-coupled respiration. The remaining OCR of 93 ± 12 – 89 ± 12 pmol/min for **1** (■+▨), 74 ± 3 – 70 ± 3 pmol/min for control (▨), accounts for uncoupled respiration. Next, the maximal uncoupled capacity was determined, which represents activation of UCP1. Isoprotenerol (Iso) is a β -adrenoceptor agonist known to activate UCP1.³⁵ At time = 40 min, iBAs were treated with 1 μM Iso, which resulted in increased OCR of 332 ± 17 – 408 ± 18 pmol/min for cells treated with synthetic **1** (■+▨) and 293 ± 11 – 352 ± 13 pmol/min for control (▨). At time = 62 min, the maximal overall respiration capacity was measured by complete chemical uncoupling of all mitochondria through the addition of trifluoromethoxy carbonyl cyanide phenylhydrazine (FCCP, 3.9 μM), leading to OCR values of 650 ± 13 – 648 ± 7 pmol/min for **1** (■) and 710 ± 8 – 657 ± 10 pmol/min for control (■+▨). Finally at time = 84, non-mitochondrial respiration (■) was determined to be 86 ± 2 pmol/min for **1** and 77 ± 1 pmol/min for control following complete chemical inhibition of mitochondrial respiration induced by the addition of a combination of rotenone (3 μM) and 3.6 μM antimycin A (Rot/Ant).

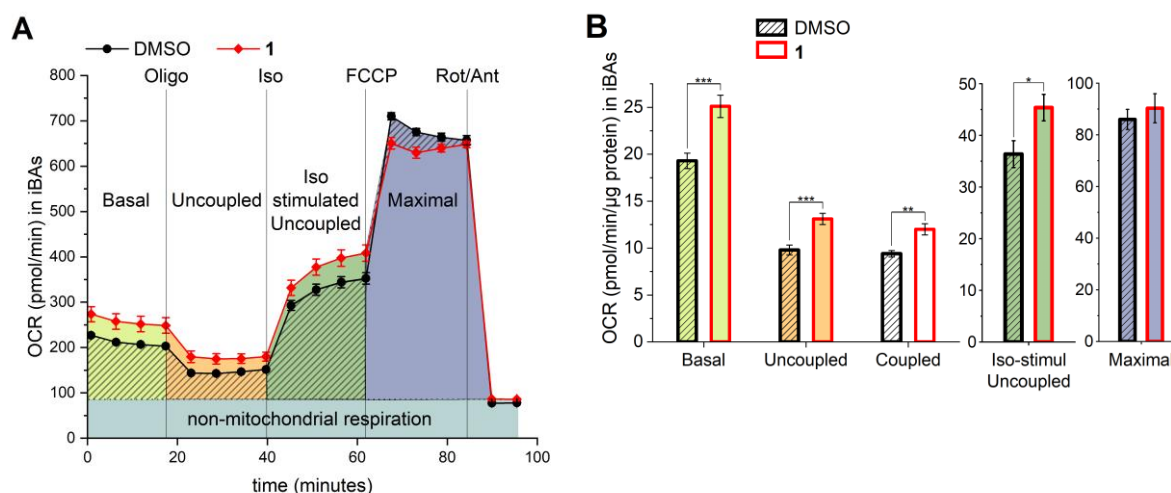


Figure 1: 1-Deacetylcaesalmin C (**1**) treatment stimulates mitochondrial respiration levels in immortalized murine brown adipocytes. Cells were treated with 10 μ M of (+)-1-deacetylcaesalmin C (**1**) for 3 days. Data are presented as mean \pm SEM. Statistical analysis was performed by two-sided Student's t-test. Significance is indicated as * p < 0.05, ** p < 0.01 and *** p < 0.001. Oligo = oligomycin; Iso = isoproterenol; FCCP = trifluoromethoxy carbonylcyanide phenylhydrazone; Rot/Ant = rotenone and antimycin.

The comparison between the normalized OCRs of iBAs treated with **1** and the OCRs of DMSO controls is shown in Figure 1B at the different stages of the Seahorse XF96 experiment. A significant increase in basal oxygen consumption was observed in the presence of **1** (25.1 \pm 1.2 pmol/min/ μ g) compared to control (19.3 \pm 0.8 pmol/min/ μ g). The contribution of uncoupled respiration was 13.1 \pm 0.6 pmol/min/ μ g for **1** and 9.8 \pm 0.5 pmol/min/ μ g for control, whereas the one of coupled respiration was 12 \pm 0.6 pmol/min/ μ g for **1** and 9.4 \pm 0.3 pmol/min/ μ g for control. Additionally, we found an increase in Iso-stimulated uncoupled respiration of 45 \pm 2.3 pmol/min/ μ g for **1** and 36 \pm 1.8 pmol/min/ μ g for control. In contrast, maximal overall respiration was not significantly altered (86 \pm 4.3 and 90 \pm 4.5 pmol/min/ μ g). In parallel experiments, cells treated with **2**–**4** displayed no relative increase compared to control (for details see SI). These results demonstrate that **1** stimulates uncoupled respiration and increases the maximal uncoupling capacity of brown adipocytes. Maximal overall respiration is not altered after treatment of iBAs with **1**, indicating that **1** is not causing changes in mitochondrial mass. The effect of 1-deacetylcaesalmin C (**1**) on uncoupled respiration is comparable to that of the state-of-the-art natural uncoupler capsaicin, which was shown to be neurotoxic.^{36,37} Stimulation of uncoupled respiration in brown adipocytes is a potential therapeutic target for obesity, because it leads to thermogenesis or release of excess energy as heat.¹⁴ All in all, these results suggest that **1** is a promising lead compound for further development to tackle obesity.

In conclusion, we report the first and enantioselective total syntheses of (+)-1-deacetylcaesalmin C (**1**), (+)- δ -caesalpin (**2**), (+)-norcaesalpinin MC (**3**) and (+)-norcaesalpinin P (**4**), enabled by a common keystone intermediate. Key steps include *exo*-selective Diels–Alder reaction and chemoselective Birch reduction to access the 6/6/6/5 carbon skeleton of cassane furanoditerpenoids. Study of oxygen consumption rates showed that (+)-1-deacetylcaesalmin C (**1**) upregulates uncoupled respiration and maximal Iso-stimulated uncoupled capacity in brown adipocytes. These findings could be useful for the development of future anti-obesity drugs. Further syntheses of related natural products and evaluation of their biological activity are ongoing and will be reported in due course.

Acknowledgements

We acknowledge Dr. Nils Trapp and Michael Solar for X-ray crystallographic analysis. Furthermore, we are grateful to Dr. Marc-Olivier Ebert, René Arnold, Rainer Frankenstein, and Stephan Burkhardt for NMR measurements. Janis Birrer is thanked for his help during scale-up.

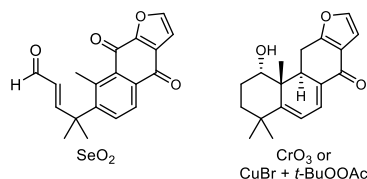
References

- (1) The INS Natural Product Libraries from IMD Natural Solutions was tested on the oxygen consumption rate in immortalized murine brown adipocytes.
- (2) Kalauni, S. K.; Awale, S.; Tezuka, Y.; Banskota, A. H.; Linn, T. Z.; Kadota, S. Methyl Migrated Cassane-Type Furanoditerpenes of *Caesalpinia crista* from Myanmar. *Chem. Pharm. Bull.* **2005**, *53*, 1300–1304.
- (3) Bernasconi, S.; Gariboldi, P.; Jommi, G.; Sisti, M.; Tavecchia, P. Synthesis of (+)-methyl vouacapenate from podocarpic acid. An improved route. *J. Org. Chem.* **1981**, *46*, 3719–3721. Spencer, T. A.; Smith, R. A. J.; Storm,

- D. L.; Villarica, R. M. Total synthesis of (+)-methyl vinhaticoate and (+)-methyl vouacapenate. *J. Am. Chem. Soc.* **1971**, *93*, 4856–4864. Feng, W.; Kazuhiro, C.; Masahiro, T. Stereoselective Synthesis of (\pm)-7 β -Acetoxypouacapanone. *Chem. Lett.* **1993**, *22*, 2117–2120.
- (4) Mahdjour, S.; Harche-Kaid, M.; Haidour, A.; Chahboun, R.; Alvarez-Manzaneda, E. Short Route to Cassane-Type Diterpenoids: Synthesis of the Supposed Structure of Benthaminin 1. *Org. Lett.* **2016**, *18*, 5964–5967. Zentar, H.; Arias, F.; Haidour, A.; Alvarez-Manzaneda, R.; Chahboun, R.; Alvarez-Manzaneda, E. Protecting-Group-Free Synthesis of Cassane-Type Furan Diterpenes via a Decarboxylative Dienone–Phenol Rearrangement. *Org. Lett.* **2018**, *20*, 7007–7010. Nakazawa, Y.; Nagatomo, M.; Oikawa, T.; Oikawa, M.; Ishikawa, Y. Studies directed toward synthesis of taapeenin D: construction of the C4 stereogenic center and the CD benzofuran rings. *Tetrahedron Lett.* **2016**, *57*, 2628–2630. Antoniou, A.; Chatzopoulou, M.; Bantzi, M.; Athanassopoulos, C. M.; Giannis, A.; Pitsinos, E. N. Identification of Gli-mediated transcription inhibitors through synthesis and evaluation of taapeenin D analogues. *Med. Chem. Commun.* **2016**, *7*, 2328–2331. Chatzopoulou, M.; Antoniou, A.; Pitsinos, E. N.; Bantzi, M.; Koulocheri, S. D.; Haroutounian, S. A.; Giannis, A. A Fast Entry to Furanoditerpenoid-Based Hedgehog Signaling Inhibitors: Identifying Essential Structural Features. *Org. Lett.* **2014**, *16*, 3344–3347. Pitsinos, E. N.; Mavridis, I.; Tzouma, E.; Vidali, V. P. Enantioselective Synthesis of Cassane-Type Furanoditerpenoids: Total Synthesis of Sucutiniranes C and D. *Eur. J. Org. Chem.* **2020**, *2020*, 4730–4742.
- (5) Canonica, L. J., G.; Mannito P.; Pagnoni U. M.; Pelizzoni F; Scolastico C. Struttura delle cisalpine. *Gazz. Chim. Ital.* **1966**, *96*, 698–720.
- (6) Balmain, A.; Connolly, J. D.; Ferrari, M.; Ghisalberty, E. L.; Pagnoni, U. M.; Pelizzoni, F. The stereochemistry of the furanoditerpenoids α -, β -, and δ -caesalpin. *J. Chem. Soc. D* **1970**, 1244–1245. Connolly, J. D.; Orsini, F.; Pelizzoni, F.; Ricca, G. ^{13}C NMR spectra of cassane diterpenoids. The stereochemistry of the caesalpines. *Org. Magn. Reson.* **1981**, *17*, 163–165.
- (7) Jiang, R.-W.; Ma, S.-C.; He, Z.-D.; Huang, X.-S.; But, P. P.-H.; Wang, H.; Chan, S.-P.; Ooi, V. E.-C.; Xu, H.-X.; Mak, T. C. W. Molecular structures and antiviral activities of naturally occurring and modified cassane furanoditerpenoids and friedelane triterpenoids from *Caesalpinia minax*. *Biorg. Med. Chem.* **2002**, *10*, 2161–2170.
- (8) Kalauni, S. K.; Awale, S.; Tezuka, Y.; Banskota, A. H.; Linn, T. Z.; Kadota, S. Cassane- and Norcassane-Type Diterpenes of *Caesalpinia crista* from Myanmar. *J. Nat. Prod.* **2004**, *67*, 1859–1863.
- (9) Liu, T.; Wang, M.; Qi, S.; Shen, X.; Wang, Y.; Jing, W.; Yang, Y.; Li, X.; Gao, H. New cassane-type diterpenoids from kernels of *Caesalpinia bonduc* (Linn.) Roxb. and their inhibitory activities on phosphodiesterase (PDE) and nuclear factor-kappa B (NF- κ B) expression. *Bioorganic Chemistry* **2020**, *96*, 103573–103580.
- (10) Tremmel, M.; Gerdtham, U.-G.; Nilsson, P. M.; Saha, S. Economic Burden of Obesity: A Systematic Literature Review. *Int. J. Environ. Res. Public Health* **2017**, *14*, 435–452. De Pergola, G.; Silvestris, F. Obesity as a Major Risk Factor for Cancer. *J. Obes.* **2013**, *2013*, 291546–291556.
- (11) Powell, A. G.; Apovian, C. M.; Aronne, L. J. New drug targets for the treatment of obesity. *Clin. Pharmacol. Ther.* **2011**, *90*, 40–51.
- (12) While writing this manuscript an anti-obesity drug has been developed, highlighting the importance for development of pharmaceutical solutions targeting obesity.
- (13) Kaukua, J.; Pekkarinen, T.; Sane, T.; Mustajoki, P. Health-related quality of life in obese outpatients losing weight with very-low-energy diet and behaviour modification: a 2-y follow-up study. *Int. J. Obes. Relat. Metab. Disord.* **2003**, *27*, 1072–1080.
- (14) Sun, W.; Modica, S.; Dong, H.; Wolfrum, C. Plasticity and heterogeneity of thermogenic adipose tissue. *Nat. Metab.* **2021**, *3*, 751–761.
- (15) Badovskaya, L. A.; Povarova, L. V. Oxidation of furans (Review). *Chem. Heterocycl. Comp.* **2009**, *45*, 1023–1034.
- (16) Jenkins, P. R.; Menear, K. A.; Barraclough, P.; Nobbs, M. S. An intramolecular Diels–Alder approach to forskolin. *J. Chem. Soc., Chem. Commun.* **1984**, 1423–1424. Magnus, P.; Walker, C.; Jenkins, P. R.; Menear, K. A. Mechanistic rationalization of an apparently non-stereospecific intramolecular Diels–Alder reaction. *Tetrahedron Lett.* **1986**, *27*, 651–654.
- (17) Tsai, Y.-F.; Peddinti, R. K.; Liao, C.-C. Intramolecular Diels–Alder reactions of masked p-benzoquinones: a novel methodology for the synthesis of highly functionalized cis-decalins. *Chem. Commun.* **2000**, 475–476.
- (18) Della Monica, C.; Della Sala, G.; D’Urso, D.; Izzo, I.; Spinella, A. Enantioselective synthesis of 1(R)-hydroxypolygodial. *Tetrahedron Lett.* **2005**, *46*, 4061–4063. Corey, E. J.; Da Silva Jardine, P.; Mohri, T. Enantioselective route to a key intermediate in the total synthesis of forskolin. *Tetrahedron Lett.* **1988**, *29*, 6409–6412.
- (19) Delpech, B.; Calvo, D.; Lett, R. Total synthesis of forskolin — Part I. *Tetrahedron Lett.* **1996**, *37*, 1015–1018.
- (20) The literature procedure was modified by conducting the ozonolysis and epoxide opening in one pot.
- (21) Tsunoda, T.; Yamamiya, Y.; Itô, S. 1,1’-(azodicarbonyl)dipiperidine-tributylphosphine, a new reagent system for Mitsunobu reaction. *Tetrahedron Lett.* **1993**, *34*, 1639–1642.
- (22) For material throughput on preparative scale the diastereomers were not separated.
- (23) Takano, D.; Nakajima, Y.; Miyahara, I.; Hirotsu, K.; Tanaka, R.; Okada, K.; Morimoto, Y.; Kinoshita, T.; Yoshihara, K. The Birch reduction of heterocyclic compounds. IV. Birch reduction of 3-acylfurans. Competition between ring reduction, carbonyl reduction, and dimer formation. *J. Heterocycl. Chem.* **1998**, *35*, 1285–1293.

(24) Massy-Westropp, R.; Warren, R. The reduction of 2-substituted furan derivatives with lithium and ammonia. *Aust. J. Chem.* **1984**, *37*, 1303–1311.

(25) To effect C7 allylic oxidation different conditions were tested but only the following side products were isolated:



(26) A ¹H NMR signal (1.12 ppm) did not match with the reported tabular value (2.11 ppm). However, ¹³C NMR spectral data were in full agreement. In addition the αD value for synthetic **4** (+68.5) did not match with the reported value (–58). CD measurements and X-ray analysis of **15** suggest a typing error in the isolation report. For further discussion see SI.

(27) Ferrarini, R. S.; Dos Santos, A. A.; Comasseto, J. V. Tellurium in organic synthesis: a general approach to buteno- and butanolides. *Tetrahedron* **2012**, *68*, 8431–8440.

(28) A ¹H NMR signal (1.71–1.84 ppm) did not match with the reported value (1.11 ppm) and a ¹³C NMR signal (32.4 ppm) did not match with the reported value (30.5 ppm). X-ray analysis of **15** and 2D NMR analysis of **3** suggest a typing error in the isolation report. For further discussion see SI.

(29) ¹H NMR signal (1.92 ppm (dd), 1.97–2.04) did not match with the reported value (2.02 ppm, 1.61 ppm) and a ¹³C NMR signal (48.7 ppm) did not match with the reported value (35.1 ppm). X-ray analysis of **14** and 2D NMR analysis of **2** suggest a typing error in the isolation report. For further discussion see SI.

(30) Liu, T.; Ning, Z.; Yin, Y.; Qi, S.; Gao, H. Acid-catalyzed transformation of cassane diterpenoids from *Caesalpinia bonduc* to aromatic derivatives. *RSC Adv.* **2021**, *11*, 22070–22078.

(31) ¹H NMR signals (1.90–2.05 ppm, 1.10 ppm) did not match with the reported value (2.89 ppm, 1.00 ppm). X-ray analysis of **15** and 2D NMR analysis of **1** suggest a typing error in the isolation report. For further discussion see SI.

(32) Gu, X.; Ma, Y.; Liu, Y.; Wan, Q. Measurement of mitochondrial respiration in adherent cells by Seahorse XF96 Cell Mito Stress Test. *STAR Protocols* **2021**, *2*, 100245–100257.

(33) Bartelt, A.; Bruns, O. T.; Reimer, R.; Hohenberg, H.; Ittrich, H.; Peldschus, K.; Kaul, M. G.; Tromsdorf, U. I.; Weller, H.; Waurisch, C.; et al. Brown adipose tissue activity controls triglyceride clearance. *Nat. Med.* **2011**, *17*, 200–205.

(34) Balazova, L.; Balaz, M.; Horvath, C.; Horváth, Á.; Moser, C.; Kovanicova, Z.; Ghosh, A.; Ghoshdastider, U.; Efthymiou, V.; Kiehlmann, E.; et al. GPR180 is a component of TGFβ signalling that promotes thermogenic adipocyte function and mediates the metabolic effects of the adipocyte-secreted factor CTHRC1. *Nat. Commun.* **2021**, *12*, 7144–7161.

(35) Miller, C. N.; Yang, J.-Y.; England, E.; Yin, A.; Baile, C. A.; Rayalam, S. Isoproterenol Increases Uncoupling, Glycolysis, and Markers of Beiging in Mature 3T3-L1 Adipocytes. *PLoS One* **2015**, *10*, 1–14.

(36) Takeda, Y.; Dai, P. Capsaicin directly promotes adipocyte browning in the chemical compound-induced brown adipocytes converted from human dermal fibroblasts. *Scientific Reports* **2022**, *12*, 6612–6625.

(37) Jancso, G.; Király, E.; Joó, F.; Such, G.; Nagy, A. Selective degeneration by capsaicin of a subpopulation of primary sensory neurons in the adult rat. *Neuroscience Letters* **1985**, *59*, 209–214.